is approximately 37.3%, 5.9%, 56.3%, 0.5%, 10^{-16}%, and 10^{-10}%, respectively. Since Se_2^{2+} obtains its highest concentration at $R = 3$, it is seen that our assumption that Se_2^{2+} is never present in high concentrations is correct. A calculation based on the potentiometric measurements at $R = 20.98_8$ (the lower limit for the calculation in Table V and VI) will show that the percentages of the proposed species Se^{IV}, Se_2^{2+}, Se_4^{2+}, Se_8^{2+}, Se_{12}^{2+}, and Se_{16}^{2+} are approximately 10^{-13}%, 10^{-5}%, 0.1%, 46.7%, 31.7%, and 21.5%, respectively. The similar values for the upper limit, $R = 28.09_4$, are approximately 10^{-17}%, 10^{-6}%, 10^{-3}%, 7.0%, 22.3%, and 70.7%, respectively. Our assumption that we are dealing with only three species in the R range 20.98_8 to 28.09_4 is therefore correct; in fact the calculations show that the lower limit could have been moved down to about 18. There is no reason, however, to believe that this should have given a different picture in Tables V and VI.

Acknowledgment. The authors wish to thank Statens teknisk-videnskabelige Forskningsråd for financial support of R.F. and for computing time at NEUCC (Northern Europe University Computing Center).

Registry No. Se^{4+}, 22541-55-5; Se_2^{2+}, 62586-31-6; Se_4^{2+}, 62586-32-7; Se_8^{2+}, 12597-34-1; Se_{12}^{2+}, 62586-33-8; Se_{16}^{2+}, 62586-34-9; Se, 7782-49-2; $SeCl_4$, 10026-03-6.

References and Notes

(1) R. Fehrmann, N. J. Bjerrum, and H. A. Andreasen, *Inorg. Chem.*, **14**, 2259 (1975).
(2) J. Barr, R. J. Gillespie, R. Kapoor, and K. C. Malhotra, *Can. J. Chem.*, **46**, 149 (1968).
(3) D. J. Prince, J. D. Corbett, and B. Garbisch, *Inorg. Chem.*, **9**, 2731 (1970).
(4) I. D. Brown, D. B. Crump, and R. J. Gillespie, *Inorg. Chem.*, **10**, 2319 (1971).
(5) R. K. McMullan, D. J. Prince, and J. D. Corbett, *Inorg. Chem.*, **10**, 1749 (1971).
(6) R. Fehrmann, N. J. Bjerrum, and H. A. Andreasen, *Inorg. Chem.*, **15**, 2187 (1976).
(7) J. H. von Barner and N. J. Bjerrum, *Inorg. Chem.*, **12**, 1891 (1973).
(8) H. A. Andreasen, N. J. Bjerrum, and C. E. Foverskov, *Rev. Sci. Instrum.*, in press.
(9) R. Fehrmann, J. H. von Barner, N. J. Bjerrum, and O. F. Nielsen, to be submitted for publication.
(10) N. J. Bjerrum, *Inorg. Chem.*, **11**, 2648 (1972).
(11) R. J. Gillespie, J. Passmore, P. K. Ummat, and O. C. Vaidya, *Inorg. Chem.*, **10**, 1327 (1971).

Contribution from the Department of Geosciences and Materials Research Laboratory, The Pennsylvania State University, University Park, Pennsylvania 16802

Crystallization of Amorphous GeS_2 and $GeSe_2$ under Pressure

MASAHIKO SHIMADA and FRANK DACHILLE*

Received February 17, 1976 AIC70127M

By subjecting amorphous starting materials of GeS_2 and $GeSe_2$ to temperatures of 300–600 °C and pressures of 0–90 kbar, three polymorphs of GeS_2 (GeS_2-I, GeS_2-II, and GeS_2-III) and three polymorphs of $GeSe_2$ ($GeSe_2$-I, $GeSe_2$-II, and $GeSe_2$-III) have been synthesized. The GeS_2-I and $GeSe_2$-I are isotypic orthorhombic phases listed in ASTM x-ray file cards 17-123 and 16-80, respectively. The GeS_2-II phase synthesized under high pressure is the phase reported by Prewitt and Young.[1] The other crystalline phases are new high-pressure phases.

Experimental Section

For the preparation of the amorphous GeS_2 and $GeSe_2$ samples, stoichiometric proportions of high-purity Ge, S, and Se (99.99% and up) were sealed in a silica tube at about 10^{-4} torr, placed in a furnace, and raised slowly in temperature to 1000–1200 °C. After its contents reacted for 5 h with occasional shaking, the sample tube was quenched in water. The resultant materials were homogeneous and amorphous to x rays. The crystallization was done in a high-pressure apparatus where the load on the sample was applied between a pair of cylindrical "anvils", each anvil having a conical taper at one end which was terminated with a small circular surface.[2] The sample was compacted into a nickel ring whose outer diameter was that of the anvil's flat; the inner diameter was about 60% of the outer diameter. The ring–sample assembly was sandwiched between two disks of platinum–10% rhodium foil. Experiments demonstrated that a uniform pressure was applied to the sample that was equal to the total load divided by the area of the anvil flat when the thickness of the ring–sample + foils sandwich was between $^1/_{22}$ and $^1/_{25}$ of the diameter of the flat.[3]

Results and Discussion

Summaries of the experimental conditions used and the results obtained with the amorphous GeS_2 and $GeSe_2$ starting materials are presented in Table I, Table II, Figure 1, and Figure 2. The x-ray powder diffraction patterns for each crystalline phase and for the amorphous materials are shown in Figures 3 and 4. It will be noted that at 300 °C in the GeS_2 system crystallization did not occur after the application of pressures up to 90 kbar for 96 h; at 400 °C crystallization was not achieved with the use of pressures above 60 kbar. Although GeS_2 remained amorphous under some of the conditions noted in Table I, the x-ray diffraction traces of the amorphous quenched products provide evidence of structural changes. For example, referring to Figure 3, trace A, which is that of the starting amorphous GeS_2, has only one broad diffuse maximum near 14° 2θ. Trace B, of a sample held at

Table I. Experimental Conditions and Results for GeS_2

Sample no.	Pressure, kbar	Temp, °C	Time, h	Result
1	30	300	68	Noncrystallized
2	30	400	68	GeS_2-II
3	30	500	41	GeS_2-II
4	40	300	41	Noncrystallized
5	40	400	46	GeS_2-II
6	40	500	46	GeS_2-II
7	50	300	46	Noncrystallized
8	50	400	69	GeS_2-II
9	50	500	69	GeS_2-II
10	60	300	69	Noncrystallized
11	60	400	69	Noncrystallized
12	70	300	69	Noncrystallized
13	70	400	69	Noncrystallized
15	80	300	70	Noncrystallized
16	90	400	70	Noncrystallized
17	90	300	70	Noncrystallized
18	0	400	70	GeS_2-I
19	20	400	96	GeS_2-II
21	20	300	96	Noncrystallized
22	10	500	96	GeS_2-II
23	10	400	96	GeS_2-II
24	10	300	96	Noncrystallized
25	0	300	72	Noncrystallized
27	60	500	44	GeS_2-II (50%) + GeS_2-III (50%)
28	70	500	39	GeS_2-III (HgI_2 type)

Table II. Experimental Conditions and Results for $GeSe_2$

Sample no.	Pressure, kbar	Temp, °C	Time, h	Result
1	0	400	24	$GeSe_2$-I
2	30	300	24	Noncrystallized
3	30	400	24	Ge_2Se_2-II (GeS_2-II type)
4	50	300	24	Noncrystallized
5	50	400	24	$GeSe_2$-II
6	0	300	23	Noncrystallized
7	60	300	23	Noncrystallized
8	60	400	23	$GeSe_2$-II (40%) + $GeSe_2$-II (60%)
9	70	300	23	Noncrystallized
10	70	400	23	$GeSe_2$-III (CdI_2 type)
11	0	500	23	$GeSe_2$-I
12	10	400	23	$GeSe_2$-II
13	20	400	23	$GeSe_2$-II
14	20	500	23	$GeSe_2$-II
15	10	500	23	$GeSe_2$-II
17	80	400	72	$GeSe_2$-III
18	40	400	72	$GeSe_2$-II
19	70	450	44	$GeSe_2$-III
20	0	600	20	$GeSe_2$-I
21	10	300	44	Noncrystallized
23	40	500	17	$GeSe_2$-II (80%) + $GeSe_2$-III (20%)
24	50	500	71	$GeSe_2$-II (50%) + $GeSe_2$-III (50%)

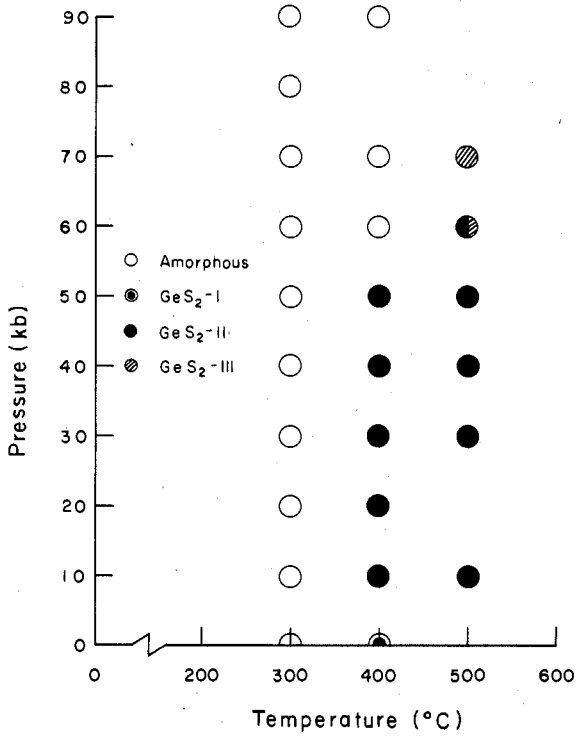

Figure 1. Results after quenching samples of amorphous GeS_2 composition.

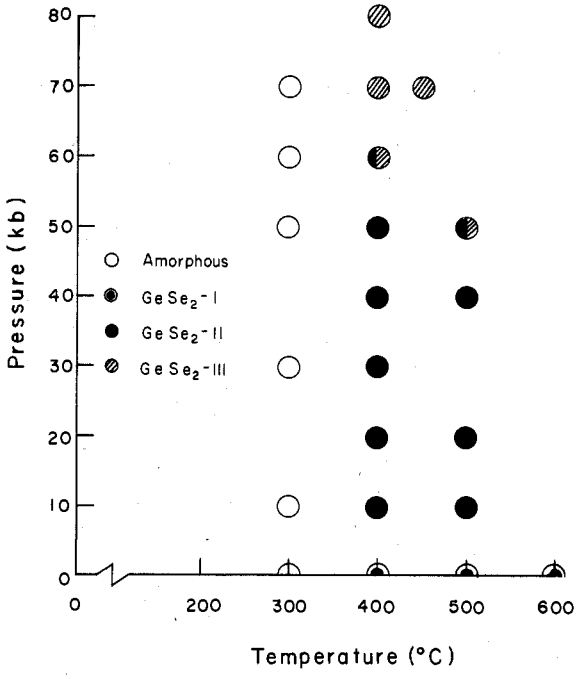

Figure 2. Results after quenching samples of amorphous $GeSe_2$ composition.

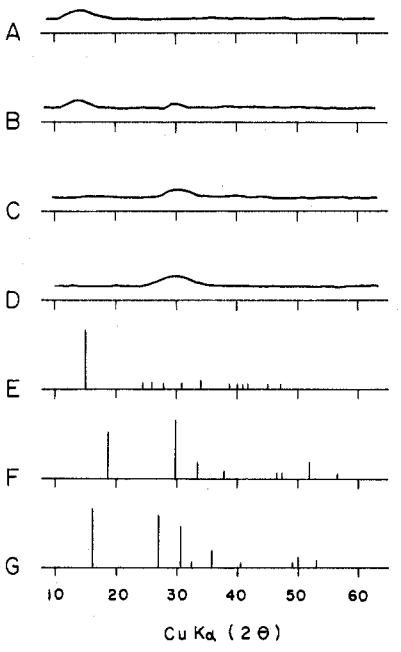

Figure 3. X-ray diffraction patterns of GeS_2 composition: A, starting material; B, 300 °C and 30 kbar for 1 h; C, 300 °C and 30 kbar for 3 h; D, 300 °C and 70 kbar for 69 h; E, GeS_2-I; F, GeS_2-II; G, GeS_2-III.

300 °C and 30 kbar for 1 h, demonstrates that a partial change from the initial amorphous state to another amorphous state has taken place; in this trace the maximum of 14° 2θ has decreased slightly while a new maximum is evident near 30° 2θ. The influence of longer heating at the same P–T conditions but for 3 h is shown in trace C where the broad diffuse maximum at 30° 2θ dominates the spectrum. The trace D, of a sample held at 300 °C and 70 kbar for 69 h, has a broad diffuse maximum of a somewhat different character near 30° 2θ.

The maxima in traces A–D appear to be precursors of maxima of planes of indices that are prominent in the crystalline phases. The schematic of GeS_2-I, trace E, should be compared with trace A; traces B and C, with both E and F; trace D, with G.

The schematic x-ray diffraction pattern of GeS_2-I is shown in Figure 2E; the d spacings and lattice parameters agree with those listed in ASTM x-ray file card 17-123 (see also ref 4): a = 6.88, b = 11.74, and c = 22.47 Å. The GeS_2-II crystallized in these experiments is identical with that described by Prewitt and Young;[1] it is a tetragonal structure with a = 5.50 and c = 9.14 Å. However, the phase that was crystallized at 500 °C and 70 kbar is a new one which has a structure closely related to the HgI_2 type; the d spacings may be indexed on a tetragonal unit cell a = 3.456 and c = 10.89 Å (Table III). The new phase is called GeS_2-III in this report. The

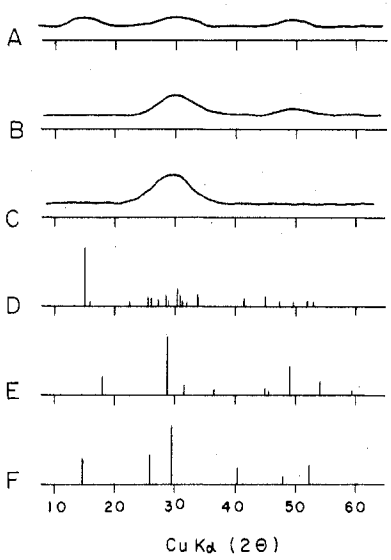

Figure 4. X-ray diffraction patterns of $GeSe_2$ composition: A, starting material; B, 300 °C and 30 kbar for 24 h; C, 300 °C and 70 kbar for 23 h; D, $GeSe_2$-I; E, $GeSe_2$-II; F, $GeSe_2$-III.

Table III. X-Ray *d* Spacings for GeS_2-III[a]

hkl	*d*(obsd)	*d*(calcd)	Intens
002	5.43	5.46	100
101	3.288	3.291	90
102	2.915	2.919	70
004	2.749	2.737	5
103	2.500	2.505	30
112	2.228	2.230	5
105	1.840	1.845	5
114	1.819	1.820	20
200	1.729	1.728	10

[a] $a = 3.456$ Å, $c = 10.89$ Å, and $d = 3.49$ g/cm³ (tetragonal structure with HgI_2-type crystal structure).

calculated densities of phases I, II, and III are 3.00, 3.29, and 3.49 g/cm³, respectively; thus GeS_2-III is 18% denser than phase I and 6% denser than phase II.

The results obtained with the $GeSe_2$ amorphous preparation are of the same general kind as for the GeS_2 sequence. Diffraction traces of schematics of amorphous and crystalline phases of $GeSe_2$ are assembled in Figure 4. The trace A of amorphous $GeSe_2$ has broad diffuse maxima at about 15, 31, and 49° 2θ. The $GeSe_2$ that was held at 300 °C and 30 kbar for 24 h yielded the diffraction trace B which appears to be in a close relationship with that of $GeSe_2$-II; presumably $GeSe_2$-II is the stable phase for the conditions if sufficient time is allowed for crystallization. Trace C is of $GeSe_2$ that was treated at 70 kbar and 300 °C for 23 h. Here, too, the pattern may be that of a precursor of the crystalline phase stable for these conditions. In this set of spectra A and D, B and E, and C and F should be viewed as closely related pairs.

Preliminary experiments had indicated that the crystallization of $GeSe_2$ would proceed more rapidly than that of GeS_2. The holding times at 300 °C were therefore set to only 1 or 2 days for the $GeSe_2$ system. As is shown in Table II and Figure 2, $GeSe_2$ remained amorphous at all applied pressures at 300 °C in this time range. Increasing the temperature to 400 °C resulted in the crystallization of the I, II, and III phases. The $GeSe_2$-I is identical with that described before;[5] it has an orthorhombic cell with $a = 6.95$, $b = 12.22$, and $c = 23.04$ Å. Similarly, the $GeSe_2$-II phase is an isotype of the GeS_2-II, and its *d* spacings can be indexed on the same tetragonal cell but with $a = 5.69$ and $c = 9.71$ Å; the *d* spacings are listed in Table IV. Treatment at pressures of 50 kbar and above resulted in the first indications of the III phase in the

Table IV. X-Ray *d* Spacings for $GeSe_2$-II[a]

hkl	*d*(obsd)	*d*(calcd)	Intens
101	4.90	4.91	30
112	3.10	3.10	100
103	2.826	2.814	15
211	2.453	2.461	10
220	2.010	2.011	15
213	2.001	2.000	5
204	1.850	1.847	50
312	1.690	1.687	25
224	1.550	1.549	5
322	1.500	1.500	5

[a] $a = 5.69$ Å, $c = 9.71$ Å, and $d = 4.87$ g/cm³ (tetragonal structure with GeS_2-II-type crystal structure).

Table V. X-Ray *d* Spacings for $GeSe_2$-III[a]

hkl	*d*(obsd)	*d*(calcd)	Intens
001	6.00	5.87	40
100	3.43	3.49	50
101	3.02	3.00	100
102	2.23	2.24	30
111	1.89	1.90	10
200	1.752	1.750	35

[a] $a = 4.03$ Å, $c = 5.89$ Å, and $d = 4.62$ g/cm³ (hexagonal structure with CdI_2-type crystal structure).

x-ray diffraction patterns of the products; after treatment at 70–80 kbar and 400–500 °C the quenched product was completely III phase. The diffraction data could be related to the CdI_2 structure type; the data are listed in Table V. Calculated densities of the I, II, and III phases are 4.70, 4.87, and 4.62 g/cm³, respectively, so that the III phase is *less* dense than the others by 1.7% and 3.0%. Although not enough data were obtained to help to establish phase boundaries, from the density relationships and the results plotted in Figure 2, it is expected that the II–III phase boundary will have a negative slope and that III is the "high-temperature" phase.

The present experiments have demonstrated that in some cases high pressures can inhibit crystallization from amorphous phases below certain temperatures. However, although the products are still x-ray amorphous, changes take place which serve to bring the amorphous structures closer to those which are assumed by the stable crystalline phases. Further, on comparing the present results with those of Prewitt and Young,[1] it is clear that GeS_2-II (and GeS_2-III) can be crystallized at lower temperatures from an amorphous composition than from stoichiometric mixtures of the elements. With due allowances for differences of compositions, the ease of crystallization of GeS_2-I, -II, and -III and of $GeSe_2$-I, -II, and -III from homogeneous amorphous phases may be compared with the experiences with the crystallization of α- and β-PbS_2[6] from mixtures under high pressure where temperatures of 900 °C or higher were necessary.

Another interesting point has to do with the difference between the GeS_2-III and the $GeSe_2$-III phases, the first being of the HgI_2 structure and the other of the CdI_2 structure; that is, an isotypic sequence of I → II → III was not followed by the two compositions to the highest pressures used. The break in the sequence may be determined in great part by the differences in the size, compressibility, and polarizability of the sulfide and selenide ions. Whatever the reasons, it can be demonstrated that the cation–anion radius ratios of HgI_2 and CdI_2, 0.51 and 0.45, respectively (with the ratio of ratios, 0.51/0.45 = 1.13), are related to those of GeS_2-III and $GeSe_2$-III. To do this it is necessary to make an approximate correction for the radii of S^{2-} and Se^{2-} in their respective III phases; the corrections are based on the density differences of the respective I and III phases. Thus if the basic radii are taken as $Ge^{4+} = 0.53$, $S^{2-} = 1.84$, and $Se^{2-} = 1.98$ Å, the latter

two are corrected to 1.74 and 1.99 Å in the III phases, with only a very small change for Ge^{4+}. The cation–anion radius ratios thus become 0.305 and 0.266, respectively, and the ratio of these ratios is 1.14. This last value is consistent with the fact that the III phases discussed in this paper are of the HgI_2 and CdI_2 structure types. Eventually, if the synthesis of analogous phases of SiS_2, $SiSe_2$, $SiTe_2$, and $GeTe_2$ should be realized, the new data will permit more specific crystal–chemical analysis of the atomic parameters which determine crystal structures.

Acknowledgment. We thank Dr. H. Hasegawa of Shizuoka University for preparing the starting materials. We also thank Dr. M. Koizumi and Dr. R. Roy for their interest in this work. This work was carried out under the auspices of JSPS Grant 4R023, NSF Grant 01P74-2195B, and Materials Research Laboratory Grant DMR 74-00340.

Registry No. GeS_2, 12025-34-2; $GeSe_2$, 12065-11-1.

References and Notes

(1) C. T. Prewitt and H. S. Young, *Science*, **149**, 535 (1965).
(2) F. Dachille and R. Roy, "High Pressure Technology", R. H. Westorf, Ed., Pergamon Press, London, 1961.
(3) M. B. Myers, F. Dachille, and R. Roy. "High Pressure Measurements", A. A. Giardini and E. C. Lloyd, Ed., Butterworths, London, 1963.
(4) Ch'un-hua et al., *Dokl. Chem. (Engl. Transl.)*, **151**, 662–664 (1963) (ASTM 17-123).
(5) Ch'un-hua et al., *Russ. J. Inorg. Chem. (Engl. Transl.)*, **7**, 1117–1119 (1962) (ASTM 16-80).
(6) M. S. Silverman, *Inorg. Chem.* **5**, 2067 (1966).

Contribution from the Department of Chemistry, Northeastern University, Boston, Massachusetts 02115

Electronic and Molecular Structure of Anhydrous Ferrous Acetate. A Weak Antiferromagnet Containing Six-Coordinate Iron(II) in Nonequivalent Environments

CHRIS CHENG and WILLIAM MICHAEL REIFF*

Received February 25, 1977 AIC70142R

The temperature and field dependence of the magnetic susceptibility and iron-57 Mössbauer spectrum of anhydrous ferrous acetate have been determined over the range 1.6–300 K. These measurements show $Fe(C_2H_3O_2)_2$ to be an extended lattice antiferromagnet (2.87 K < T_{Neel} < 3.22 K) rather than a molecular dimer. Chemical isomer shift and quadrupole splitting data and near-infrared–visible optical spectra give strong evidence for a distorted FeO_6 chromophore. Zero-field high-temperature Mössbauer spectra as well as the high-field (up to 80 kG) spectra at 4.2 K clearly show the ferrous ion present in two inequivalent environments. For an applied field of 45 kG at 4.2 K the effective internal hyperfine field at these sites is ca. 230 kG. As expected x-ray powder patterns indicate that $Fe(C_2H_3O_2)_2$ is not isomorphorus with the corresponding $Cu(C_2H_3O_2)_2$ where the susceptibility of the latter compound has been redetermined to ~50 K.

Introduction

For a number of years there has been considerable interest in the chemistry of the acetates of first transition series divalent metal ions. Copper[1] and chromium[2] acetate monohydrate exist as a dimer $[M(C_2H_3O_2)_2 \cdot H_2O]_2$ which contains four bridging acetate groups. This results in a five-coordinate MO_4O' chromophore. There is ample evidence for magnetic exchange interaction between such chromophores in the dimer. However, some question arises as to whether exchange is indirect δ-symmetry superexchange via the bridging carboxylate groups or is through direct δ interaction of the metals.[3]

Our initial interest in anhydrous ferrous acetate arose from its use as a precursor for a number of other ferrous complexes. A check of the literature shows that there has been relatively little study[4] of this compound, probably owing to its instability in air. We have thus set out to characterize $Fe(C_2H_3O_2)_2$ insofar as we can, short of a single-crystal x-ray study.

Experimental Section

Anhydrous ferrous acetate can be synthesized directly by dissolving iron metal in glacial acetic acid under anaerobic conditions.[4] It can also be purchased in relatively pure form (pale buff-colored powder) from chemical supply houses packed under argon. A sample of this type was obtained from Alfa Inorganics Co. (Alfa No. 31140) and gave the following analyses: observed by the manufacturer, % C = 27.94, % H = 3.64 (calculated % C = 27.60, % H = 3.48, % Fe = 32.11); observed by Galbraith Laboratories, % C = 28.19, % H = 3.70, % Fe = 30.91 (ash). Anhydrous cupric acetate was prepared by dehydration of $Cu(C_2H_3O_2)_2 \cdot H_2O$ in a high-vacuum thermolysis apparatus at ~120 °C (<1 μ). For all of the experiments to be discussed, neat polycrystalline samples of $Fe(C_2H_3O_2)_2$ were kept in an evacuated atmosphere or under nitrogen or helium. Near-infrared visible optical spectra were obtained on a Cary 14 spectrometer for KBr pellets and fluorocarbon grease mulls in which decomposition was minimal. X-ray powder measurements were also made for samples under protective grease coating using a General Electric Co. XRD-6 powder diffractometer.

Variable-temperature magnetic susceptibility measurements were made at Northeastern University on a Faraday balance composed of a Cahn RG electrobalance, a Varian Model 4000 electromagnet with 4-in. constant-force pole caps and a Janis Super Vari-Temp cryostat over the range 1.5–300 K for ten fields between 1.6 and 5.1 kG. Temperature measurement and control were typically of the order ±0.01 K or better and were achieved using a Leeds-Northrup K-5 potentiometer and a Lake Shore Cryotronics Model DT-500 C set point controller, respectively, in conjunction with a calibrated silicon temperature sensor diode, a 10-μA constant-current source and an uncalibrated gallium arsenide control diode. Final temperature equilibration and stability were continuously monitored on a Leeds-Northrup Speedomax-XL 600-mV recorder that was used to read the error signal of the calibrated silicon diode after cancelation by the K-5 potentiometer. Temperatures below 4.2 K were measured via a vapor pressure of helium using Wallace-Tiernan Models FA-160 and 61-050 absolute-pressure gauges while pumping was precisely controlled with an L. J. Engineering Model 329 vacuum regulator valve. Temperatures below 78 K and to as low as 50 K were also achieved using liquid nitrogen by pumping (Welch 1397) to well below the triple point on solid nitrogen. Both the vapor pressure of nitrogen and a calibrated silicon diode were used to monitor the temperature. An F. W. Bell Model 610 gaussmeter with a transverse Hall probe was used for measurement of magnetic fields. The balance was calibrated with $HgCo(NCS)_4$.[5,6]

High-field Mössbauer spectra at 4.2 K were determined at the Francis Bitter National Magnet Laboratory using a niobium–tin superconducting solenoid with the magnetic field parallel to the direction of γ-ray propagation.

Mössbauer spectra in the vicinity of 4.2 K were obtained on a conventional constant-acceleration spectrometer operated in the time mode using a γ-ray source of 100-mCi ^{57}Co in a rhodium metal matrix. Temperature control was achieved using an uncalibrated silicon diode coupled to a Lake Shore Cryotronics Model DT-500 C set point controller. Temperature measurements were made with a Leeds-Northrup K-4 potentiometer or a 6-place Dana Model 5330 digital